Design Principle of Mixed-Wettability Surfaces for Inducing Droplet Directional Rebound

ZHANG Tongwei[1], *KAKU Chuyo*[2], *LI Meixuan*[3], *WU Jie*[3,4*]

1. School of Automotive and Traffic Engineering, Jiangsu University, Zhenjiang 212013, P. R. China;
2. R&D Center, Jiangsu Chaoli Electric Co. Ltd., Zhenjiang 212321, P. R. China;
3. College of Aerospace Engineering, Nanjing University of Aeronautics and Astronautics, Nanjing 210016, P. R. China;
4. National Key Laboratory of Science and Technology on Aerodynamic Design and Research, Northwestern Polytechnical University, Xi'an 710072, P. R. China

(Received 22 March 2023; revised 12 April 2023; accepted 24 April 2023)

Abstract: Directional rebound of droplet impacting on solid surfaces is of great significance in engineering applications such as anti-icing/fogging and self-cleaning. Mixed-wettability surfaces have been shown to be as an effective way for droplet manipulation. The impact of droplet on hydrophobic substrate decorated with a hydrophilic stripe is investigated numerically. The validated diffuse interface method is adopted for interface capture. First, the formation of satellite droplets during the impact process is explored, and the role of mixed-wettability surfaces in the droplet spreading, retraction and rebound stages is clarified by analyzing the vertical and lateral velocities of the droplet. After that, the effect of the stripe width on the droplet rebound form and the contact time is studied systematically. Special attention is paid to the mechanisms of dynamics and energy transfer during the evolution of liquid film and droplet bouncing. The obtained results can provide useful guidance for the design of mixed-wettability surfaces and further optimize the control of droplet directional rebound.

Key words: droplet impact; mixed-wettability surfaces; directional rebound; design principle

CLC number: O35 **Document code:** A **Article ID:** 1005-1120(2023)02-0159-10

0 Introduction

Droplet impacting onto solid surfaces is a ubiquitous and important phenomenon in industrial processes, such as spray cooling, inkjet printing, self-cleaning and fluid transportation[1-6]. One of the key factors affecting the dynamic behavior of droplets is the surface wettability, and the droplets generally tend to rebound from the hydrophobic surfaces and adhere to the hydrophilic surfaces. Extensive works mainly focused on the contact time t_c and spreading diameter of the droplet, which may produce a marked effect on the industrial process. In general, it is advantageous to reduce the contact time between the droplet and the surface, since it controls the exchange of mass, momentum and energy[7-9]. For example, rapid droplet detachment can effectively reduce the heat exchange and suppress the ice nucleation, thus preventing the aircraft and wire from icing at low temperature. Richard et al.[8] found that t_c only scales with the inertia-capillarity time $\tau=\sqrt{\rho_1 R_0^3/\sigma}$, where ρ_1 and R_0 are the density and the initial radius of the droplet, respectively, and σ is the surface tension coefficient. The theoretical limit of t_c/τ is approximately equal to 2.2 when the droplet undergoes the spread-retraction-rebound stage on flat superhydrophobic surfaces. Recently, the researchers reported that adding single or array structures on surfaces can reduce the contact time by 37%—80%, such as pancake bouncing[10].

*Corresponding author, E-mail address: wuj@nuaa.edu.cn.

How to cite this article: ZHANG Tongwei, KAKU Chuyo, LI Meixuan, et al. Design principle of mixed-wettability surfaces for inducing droplet directional rebound[J]. Transactions of Nanjing University of Aeronautics and Astronautics, 2023, 40(2): 159-168.

http://dx.doi.org/10.16356/j.1005-1120.2023.02.005

Although the contact time can be reduced by the chemical or physical treatments of the surface, the droplets usually rebound along the original route (in a perpendicular type). This may limit its engineering applications, since the droplets will eventually fall back and adhere to the horizontal surface with the dissipation of kinetic energy. Therefore, the demand for droplet rebound with lateral motion (deflection) emerges, and many attempts have been made in this aspect. The intuitive idea is to exert a lateral force on the droplet during the rebound process, such as introducing the wind-driven, electric or magnetic fields[11-14]. However, these methods with external power input are sometimes unstable and hard to control. Recently, the use of engineering surfaces, such as roughness gradient, wettability gradient and bioinspired structures, to realize the spontaneous lateral motion of droplets has attracted wide attention[15-18].

The development of mixed-wettability surfaces provides a fresh insight into the droplet manipulation, since the forces exerted on various wettability partitions are different. Farshchian et al.[19] reported a directional rebounding phenomenon when the droplet impacted on the borderline between the hydrophobic and hydrophilic portions of a heterogeneous surface. The experimental results showed that the lateral transportation distance can increase with the Weber number (We) in the range of 3.2 to 18.9. Chu et al.[20] further investigated the effect of impacting offset position on the deflection distance at higher We. The maximum lateral transportation distance can be up to 13 times longer than the droplet diameter. In these studies, the nonorthogonal rebound of the droplet is realized by impacting on the junction region of a dual-textured substrate, and the lateral motion is mainly caused by asymmetric forces generated at the retraction stage. Based on this mechanism, the researchers tried to adopt the hydrophobic substrate decorated with hydrophilic patterns to control the droplets. Schutzius et al.[21] and Zhao et al.[22] designed a hydrophilic "arc" and "stripe" on a superhydrophobic surface, respectively. The impacting droplet could rebound toward the direction of the hydrophilic patterns instead of orthogonal to the surface. Then the simple practical applications were achieved by the well-controlled droplet motion, such as the on-demand chemical reaction system and droplet-driven micro-boat system. Furthermore, Li et al.[23] realized more various rebound behaviors of the droplets, such as gyration, rolling, and deflection, by using the heterogeneous surfaces with different high-adhesion (hydrophilic) patterns. In addition to experimental studies, Russo et al.[24] and Zhang et al.[25] recently numerically investigated the droplet impacting on a wettability-patterned surface. The numerical method coupled with the Kistler dynamic contact angle model and adaptive mesh-refinement technique was fully validated, and the dynamic mechanisms of droplet rebound were revealed by analyzing the variation of the contact line and velocity profile.

In the abovementioned studies, various forms of hydrophilic patterns were designed, and the results showed that their effects on the dynamic behavior of droplets were nonlinear and complex. Taking the distance a between the impacting point and hydrophilic pattern as an example, the lateral velocity v_x of the droplet continuously increases with a for the arc-shaped pattern, while v_x increases first and then decreases with the increase of a for the stripe-shaped pattern. To clarify the relationship between hydrophilic patterns and the droplet lateral motion, the parameter of "effective retraction area" S is proposed to quantify the geometric parameters and position of different patterns in our previous work[25]. Furthermore, we systematically investigated the effects of multiple parameters on the dynamic behaviors of the droplet impact, and some scaling laws for droplet rebound with the lateral motion were proposed[26]. Thus, the prediction and control of droplet directional rebound were preliminarily achieved. However, the design principle of mixed-wettability surfaces has never been established due to the following two problems. First, small satellite droplets may form during the impact process, which has occurred in both experimental observations and numerical simulations, but has not received much attention[21, 24]. The energy transfer characteristics between the main and satellite droplets are not known

yet, so the role of mixed-wettability surfaces in the formation of satellite droplets remains unclear. Second, although various forms of hydrophilic patterns have been studied in previous works, they were all carried out when the width of patterns was about 10% of the droplet diameter. It is not clear whether a better pattern width exists for droplet directional rebound. And the effect of the size (width) of the hydrophilic pattern on the adhesive force and droplet rebound modes (partial and complete rebound) is also unidentified. Therefore, the above two significant factors need to be further explored to establish the universal design principle.

In this paper, the impacting dynamics of the droplet on mix-wettability surfaces (hydrophobic substrate decorated with a hydrophilic stripe) are simulated by a reliable numerical method. The role of the hydrophilic stripe in the satellite droplet formation is clarified, and the dynamic and energy transfer mechanisms of the directional rebound of the main droplet are revealed. Then, the effect of the width of the hydrophilic stripe on adhesive force, liquid residual and rebound modes is systematically studied. On this basis, the comprehensive design principle of mix-wettability surfaces for inducing directional rebound is proposed, which provides valuable guidance for the droplet manipulation.

1 Problem Description and Methodology

The sketch of droplet impact is illustrated in Fig.1. The mixed-wettability surface is consisted of two parts: The superhydrophobic substrate (yellow region) and the hydrophilic stripe (red region). The droplet with diameter D_0 is initially very close to the surface, and it impacts the surface with a predetermined impact velocity U_0. The water and air are adopted as the working fluids. The size of the computational domain is taken to be $10D_0\times10D_0\times10D_0$ so as to guarantee that the results are not affected by the boundaries, and the gravity acceleration $\boldsymbol{g}$ acts in the negative z direction. In addition, the width of the hydrophilic stripe is w. In this paper, the impact

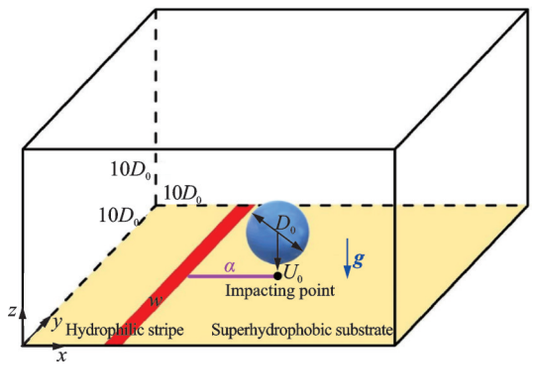

Fig.1 Sketch of the droplet impacting on a mixed wettability surface

velocity is in the range of [1.25 m/s, 2.08 m/s] and the droplet diameter is 2 mm. Since the droplet motion is mainly dominated by the surface tension and inertial forces, the dimensionless parameter of We is considered and defined as $We=\rho_l D_0 U_0^2/\sigma$. Here, ρ_l is the density of the water droplet.

The droplet-solid interaction is considered as incompressible and isothermal multiphase flow problem in this paper. The evolution of water-air interface is captured by an improved diffuse interface (DI) method, which has been implemented in the OpenFOAM framework[27]

$$\frac{\partial C}{\partial t}+\nabla\cdot(\boldsymbol{u}C)+\nabla\cdot\left[\gamma C(1-C)\frac{\nabla C}{|\nabla C|}\right]=M\nabla^2\phi \tag{1}$$

where C is the order parameter in the range of [0, 1] and $\boldsymbol{u}$ the fluid velocity. γ is an adaptive parameter used to control the magnitude of the interface-correction term, which can improve the interface sharpness. In addition, the correction term is only taken into account in the diffuse layer, and it works normal to the interfaces, i.e., in the direction $\frac{\nabla C}{|\nabla C|}$. M is the mobility and ϕ the chemical potential. Based on the free energy density model[28-29], the chemical potential is defined as $\phi=\frac{\alpha\sigma}{2\varepsilon}C(C-1)(2C-1)-\alpha\sigma\varepsilon\Delta C$. Here, ε measures the interface thickness, and α is a positive constant, which is equal to $6\sqrt{2}$[30-31]. The equilibrium function of the one-dimensional interface profile C can be written as

$$C(z_d)=\frac{1}{2}\left[1+\tanh\left(\frac{z_d}{2\sqrt{2}\,\varepsilon}\right)\right] \tag{2}$$

where z_d is the signed normal distance to the interface.

The flow field is obtained by solving the Navier-Stokes equations, which are written as

$$\nabla\cdot\boldsymbol{u}=0 \tag{3a}$$

$$\frac{\partial(\rho\boldsymbol{u})}{\partial t}+\nabla\cdot(\rho\boldsymbol{u}\boldsymbol{u})=-\nabla p+\nabla\left[\mu\cdot\left(\nabla\boldsymbol{u}+(\nabla\boldsymbol{u})^{\mathrm{T}}\right)\right]+\rho\boldsymbol{g}+\boldsymbol{F}_\sigma \tag{3b}$$

where $\boldsymbol{F}_\sigma=-C\nabla\phi$ is the surface tension force. ρ and μ are the density and the dynamic viscosity, respectively, which depend on the order parameter C

$$\rho=\rho_l C+\rho_g(1-C),\ \mu=\mu_l C+\mu_g(1-C) \tag{4}$$

where the subscripts "l" and "g" denote the water and air, respectively.

When the two-phase interface interacts with the solid surface, the unit normal vector of the interface $\boldsymbol{n}$ should be modified by the contact angle θ_d, and it is expressed as

$$\boldsymbol{n}=\frac{\nabla C}{|\nabla C|}=\boldsymbol{n}_w\cos\theta_d+\boldsymbol{t}_w\sin\theta_d \tag{5}$$

where $\boldsymbol{n}_w$ and $\boldsymbol{t}_w$ are the unit normal and tangential vectors of the solid surface, respectively. In addition, when the contact line moves on the solid surface, the contact angle is no longer a constant due to the phenomenon of the contact angle hysteresis. In this paper, the variation of the contact angle in the impacting process is predicted by the Cox-Voinov model[32], which is given in the form as

$$\theta_{num}^3=\begin{cases}\theta_{app}^3-9Ca\ln\left(\dfrac{2K}{\chi}\right) & 0\leqslant\theta_{app}\leqslant\dfrac{3\pi}{4}\\ (\pi-\theta_{app})^3+2.25\pi\ln\left(\dfrac{1-\cos\theta_{app}}{1+\cos\theta_{app}}\right)-9Ca\ln\left(\dfrac{2K}{\chi}\right) & \dfrac{3\pi}{4}<\theta_{app}\leqslant\pi\end{cases} \tag{6}$$

where θ_{app} is the apparent contact angle; $Ca=\mu_l u_{cl}/\sigma$ is the capillary number, here u_{cl} is the contact line velocity; $K=\sqrt{\sigma/\rho g}$ is the capillary length; χ denotes the grid size. Here, θ_{app} is obtained with Kistler' law[33], which is defined as

$$\theta_{app}=f_{Hoff}\left[Ca+f_{Hoff}^{-1}(\theta_e)\right]$$

and

$$\theta_e=\begin{cases}\theta_{adv} & u_{cl}>0\\ \theta_{sta} & u_{cl}=0\\ \theta_{rec} & u_{cl}<0\end{cases} \tag{7}$$

where θ_{adv}, θ_{sta} and θ_{rec} are the advancing, static and receding contact angles, respectively. The Hoffman's function f_{Hoff} can be written as

$$f_{Hoff}(x)=\arccos\left\{1-2\tanh\left[5.16\left(\frac{x}{1+1.31x^{0.99}}\right)^{0.706}\right]\right\} \tag{8}$$

The Cox-Voinov dynamics contact angle model has extensively been used in the research of the droplet impact[26, 32, 34]. It can accurately predict the variation of the contact angle in the impacting process and obtain satisfactory numerical results.

The governing equations are discretized by the finite volume method. The detailed discretization procedure can be found in our previous work[26]. In addition, the adopted numerical model and grid independence have been well-validated by simulating the problems of droplet impacting on homogeneous and heterogeneous wettability surfaces[25]. Thus, the details are not presented in this paper.

2 Results and Discussion

In this section, the directional rebound of droplet impacting on mix-wettability surfaces is numerically investigated. The attention is focused on the formation of satellite droplets and the rebound mode of the main droplet. And the design principle of mix-wettability surface is proposed for better droplet manipulation. It should be noted that the effects of multiple parameters on the droplet directional rebound have been systematically investigated in our previous works[25-26], including the Weber number (droplet diameter and impact velocity), the arrangement of hydrophilic stripes (position and shape), and the values of contact angles. The obtained results show that the droplet deposits on the surface at $We\leqslant 5$, and the droplet splashes at $We\geqslant 120$. The droplet rebound usually occurs when the Weber number is

in the range of 10 to 100. Therefore, the Weber numbers of 100 and 120 are selected to explore the droplet breakup in this paper, and a moderate value of We=43.3 is adopted to study the droplet rebound with lateral motion under various stripe widths. In addition, all cases are limited in the given contact angles. The advancing, static and receding contact angles on the hydrophobic part are set as 164°, 162°, and 160°, respectively, and the corresponding contact angles on the hydrophilic part are 120°, 80°, and 40°, respectively. The distance a between the impacting point and hydrophilic stripe is 1.5 mm.

2.1 Formation of satellite droplets

The formation of satellite droplets after impact is a well-known phenomenon. In order to explore the dynamic characteristics in this process, the droplet impacting on superhydrophobic and mixed-wettability surfaces are carried out, respectively. The evolutions of the liquid film for the cases of We=120 (D_0=2 mm and U_0=2.08 m/s) and w=0.2 mm are plotted in Fig.2. After the droplet reaching its maximum spread (t=2 ms), it starts to retract under the action of superhydrophobic substrate. It can be seen that the liquid film on homogeneous surface moves uniformly and radially towards the impacting point, and no satellite droplets are formed in the retraction stage. On the mixed-wettability surface, the right liquid film can retract normally, but the left liquid film gets pinned by the hydrophilic stripe. This prevents the central liquid film from being fully filled, causing the liquid film to thin and form holes (t=5 ms). Finally, small satellite droplets are generated with the breaking of the liquid film.

In addition, we can observe that there also are satellite droplets when the droplet rebound from the superhydrophobic surface (t=6.5 ms), as shown in Fig.2(a). To further reveal the mechanisms of dynamics and energy transfer, the morphology of bouncing droplet is shown in Fig.3(a). The result of the mixed-wettability surface is also presented for comparison. Here, the impact parameters are set as: We=100 (D_0=2 mm and U_0=1.9 m/s) and w=0.4 mm. The iso-surface is colored by the vertical velocity U_z. When the droplet rebounds from the superhydrophobic surface (t=8 ms), it is obvious that the gradient of the vertical velocity is larger than that from the mixed-wettability surface. As a result, the top liquid film is elongated and eventually separated from the main droplet. As shown in Fig.3(b), the liquid film retracts uniformly on the homogeneous surface, so the droplet rebounds vertically and the lateral velocity is $U_x\approx0$. However, the liquid film is pinned by the hydrophilic stripe of the mixed-wettability surface, and the rebound kinetic energy of the droplet is partially converted to the lateral direction. Thus, the bouncing droplet has the considerable lateral velocity.

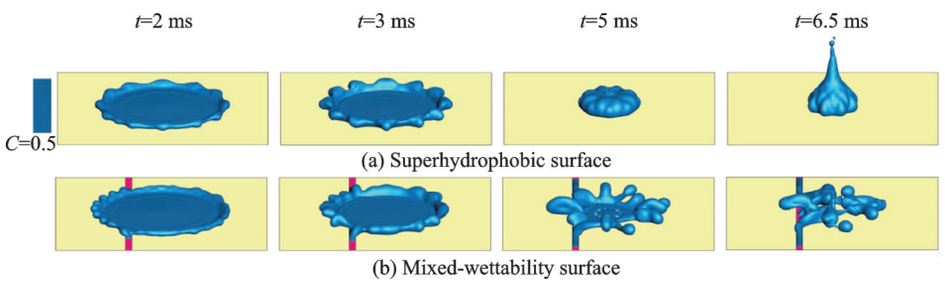

Fig.2 Time evolution of the droplet impacting on superhydrophobic and mixed-wettability surfaces

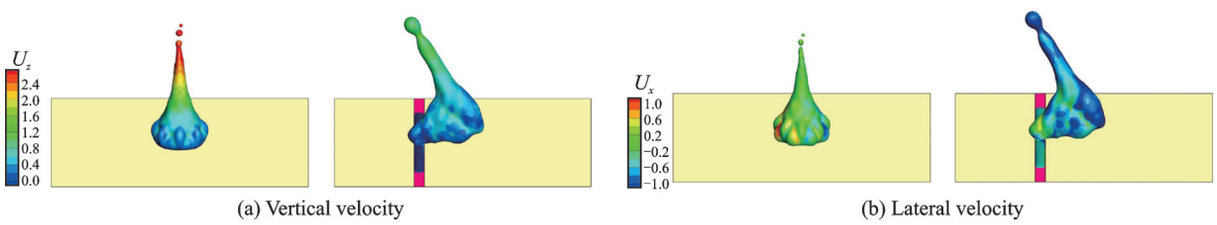

Fig.3 Morphology of the droplet rebound from superhydrophobic and mixed-wettability surfaces

The formation of satellite droplets is related to two types of instability. One is the Kelvin-Helmholtz instability in the droplet spreading and retraction stages[35]. The liquid film is thin and further forms the hole, which will cause the droplet to break. For example, the formation of satellite droplets in Fig.2(b) occurs at the central liquid film, which is caused by the adhesion of the hydrophilic stripe in the retraction stage. Similarly, the splash may occur when the droplet impacts with a large Weber number, which is induced by the liquid film breaking at the edge of spreading droplet. The other is the Plateau-Rayleigh instability in the droplet rebound stage[36]. The rebound droplet is elongated under the action of the gradient of the vertical velocity, and excessive elongation will break the liquid film and generate the satellite droplets. Especially on the superhydrophobic surface, two or three satellite droplets may appear during the droplet rebounding process. For the mixed-wettability surface, we conclude that it can suppress the Plateau-Rayleigh instability in the droplet rebound stage, but promote the Kelvin-Helmholtz instability in the droplet retraction stage. No obvious effect is observed in the droplet spreading stage.

2.2 Effects of stripe width

In this subsection, the effect of the width of the hydrophilic stripe on the droplet rebound is studied. The value of Weber number is given as 43.3, and the stripe width w varies in the range of [0.1 mm, 1.6 mm].

The evolutions of droplet rebounds from the mixed-wettability surfaces with different stripe widths are shown in Fig.4. In each case, the time t from left to right is 2, 7, 9, 12, 15, and 18 ms. It can be seen that the rebound form and contact time of the droplet vary greatly under different widths. For the case of w=0.1 mm, the droplet leaves the surface immediately after retraction. The low adhesion exerted by the narrow stripe is not sufficient to hold the droplet, causing the droplet to rebound completely without the liquid residue. For the cases of w=0.3 mm and 0.8 mm, a liquid bridge is formed between the rebound droplet and the residual liquid film. In the process of the lateral rebound, the liquid bridge is broken and the droplet leaves the surface. It should be noted that the "separate angle" of the droplet (marked with black lines in Figs.4(b,

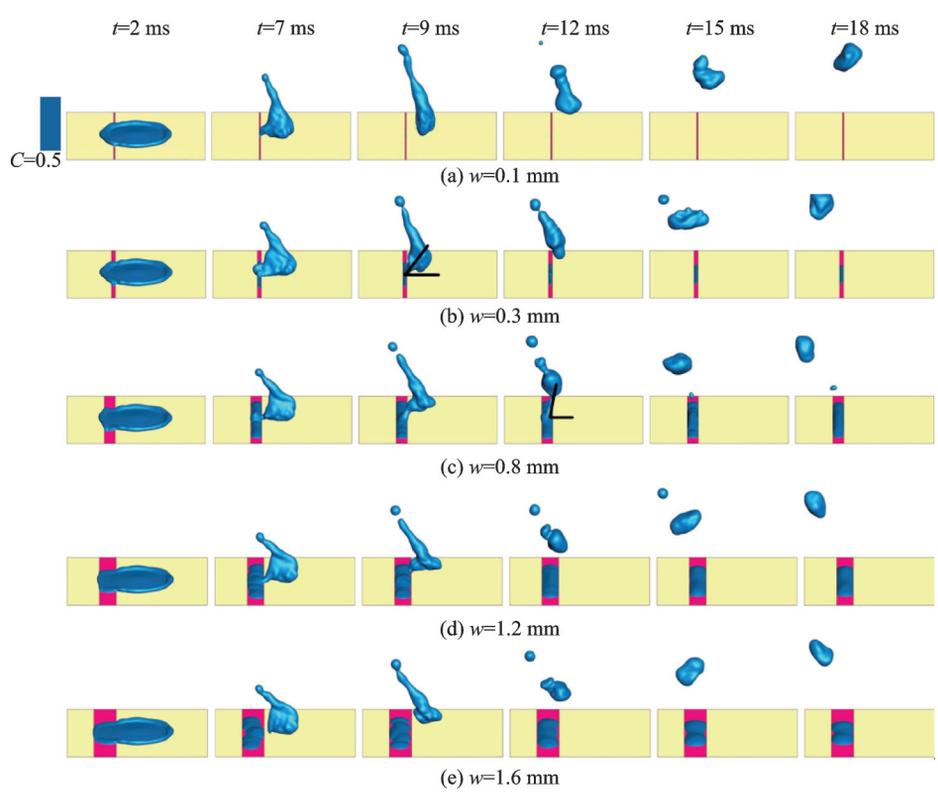

Fig.4 Evolutions of droplet rebounds from the mixed-wettability surfaces with different stripe widths

c) is different, which determines the contact time. With the further increase of the stripe width (w= 1.2 mm and 1.6 mm), the droplet leaves the surface immediately after retraction, which is similar to the case of w=0.1 mm. On the contrary, the high adhesion exerted by the wide stripe breaks the connection between the droplet and the liquid film, and a large amount of liquid remains on the hydrophilic stripe.

For the above three typical rebound forms of the droplet, the variation of the contact time with the stripe width is shown in Fig.5. The separation of droplet is mainly determined by the inertial force (rebound) and the surface tension force (adhesion). In the phases of ① and ③, the inertial force and the surface tension force are dominate, respectively. Thus, the droplet can rebound from the surface rapidly, and the contact time is about 8 ms, which is similar to that of the droplet impacting on the superhydrophobic surface (w=0). In the phase of ②, the contact time increases first and then decreases, which is related to the evolution of liquid bridge. For the small stripe width, the broken liquid bridge will leave the surface together with the rebound droplet. With the increase of w, the adhesion of the hydrophilic stripe is enhanced, and the broken liquid bridge tends to remain on the surface. Here, the maximal contact time is obtained when the stripe width is 0.8 mm.

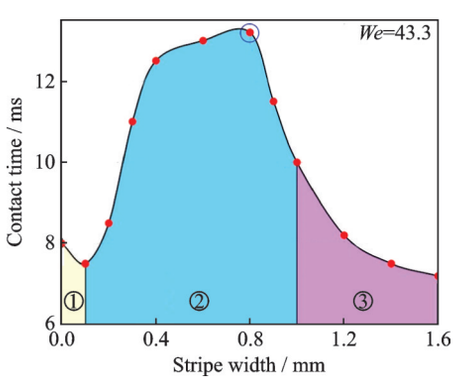

Fig.5 Variation of the contact time with the stripe width

2.3 Design principle

For the droplet directional rebound, three factors need to be considered in the design of the mixed-wettability surface, including the formation of satellite droplets, the lateral velocity of the rebound droplet and the liquid residue on the hydrophilic stripe. Among of them, the situations of satellite droplets and the liquid residue can be easily obtained from the above results. When the Weber number is in the range of [10, 100], the mixed-wettability surface can suppress the formation of the satellite droplets in the rebound stage. However, it may induce the Kelvin-Helmholtz instability at the higher Weber number, thus promoting the formation of satellite droplets. In addition, the liquid residue is usually unfavorable in engineering applications, such as the anti-icing/fogging and self-cleaning. Fig.6 shows the percentage of residual liquid in the total mass of droplets. It is clear that the liquid residue increases with the stripe width.

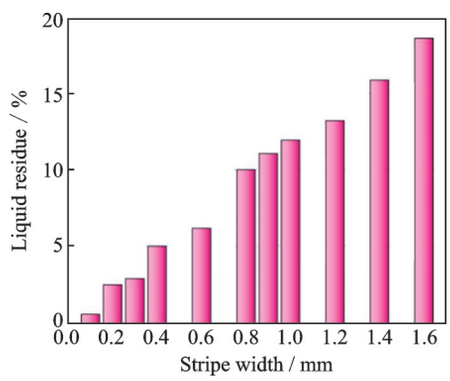

Fig.6 Variation of the liquid residue with the stripe width

This subsection focuses on the effect of the stripe width on the performance of the droplet directional rebound. The kinetic energy E_k of the droplet rebound from the mixed-wettability surface with different stripe widths are shown in Fig.7. The impacting droplet undergoes the spreading, retraction and rebound stages, in which part of the energy dissipates due to the surface friction and viscosity. It can be seen that the variation trend of rebounding kinetic energy is opposite to that of contact time (Fig.5). This is mainly because the longer the droplet is pulled by the hydrophilic stripe, the more energy it loses during its movement. Therefore, the minimum kinetic energy is obtained at w=0.8 mm, which corresponds to the maximum contact time.

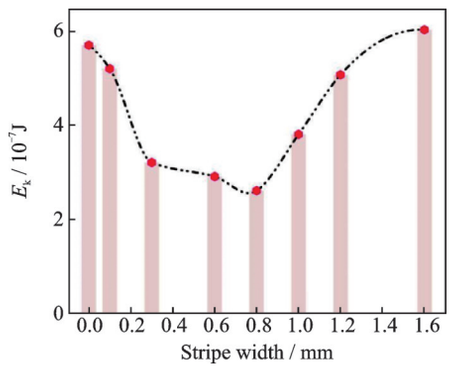

Fig.7 Variation of the rebounding kinetic energy E_k with the stripe width

Furthermore, the effect of the stripe width on the rebounding height H and the lateral velocity v_x of the droplet is shown in Fig.8. The lateral velocity can quantify the performance of droplet directional transportation, and the variation trend of v_x is similar to that of contact time (Fig.5). This means that the energy continually transfer laterally before the droplet leaves the surface. The high lateral velocity can be obtained when the stripe width is in the range of [0.3 mm, 1.2 mm]. With the increase of the contact time, more energy is lost during the impact process and the more energy is transferred to the lateral direction. Thus, it is easily understood that the droplet rebounding height H is lower at the medium stripe width.

In summary, two principles can be obtained to provide reference for the design of mixed-wettability surfaces. Firstly, the mixed-wettability surface is more suitable for the droplet directional rebound with Weber number between 5 and 100. In this range, the existence of the hydrophilic stripe can effectively suppress the formation of satellite droplets.

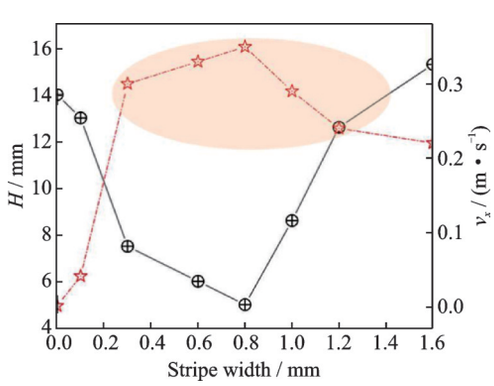

Fig.8 Variations of the rebounding height H and the lateral velocity v_x with the stripe width

Secondly, w=0.3 is a better choice for the purpose of obtaining the larger rebounding kinetic energy, the higher lateral velocity and the lesser liquid residue.

3 Conclusions

The dynamics of a droplet impacting on the mixed-wettability surface, which can induce the directional rebound, are systematically investigated. The numerical results show that the mixed-wettability surface can effectively suppress the formation of the satellite droplets in the rebound stage, but promote the Kelvin-Helmholtz instability in the retraction stage. Moreover, three typical droplet rebound forms are observed with different stripe widths. The larger lateral velocity and rebounding kinetic energy of the droplet, and the less liquid residue on the hydrophilic stripe can be obtained when w=0.3 mm. These results may be useful for the design of the mixed-wettability surface, thus further promoting its application in engineering.

References

[1] LOHSE D. Fundamental fluid dynamics challenges in inkjet printing[J]. Annual Review of Fluid Mechanics, 2022, 54: 349-382.

[2] LI J, QIN Q, SHAH A, et al. Oil droplet self-transportation on oleophobic surfaces[J]. Science Advances, 2016, 2: e1600148.

[3] LV J, SONG Y, JIANG L, et al. Bio-inspired strategies for anti-icing[J]. ACS Nano, 2014, 8: 3152-3169.

[4] JIANG M, WANG Y, LIU F, et al. Inhibiting the Leidenfrost effect above 1 000 ℃ for sustained thermal cooling[J]. Nature, 2022, 601: 568-572.

[5] LU Y, SATHASIVAM S, SONG J, et al. Robust self-cleaning surfaces that function when exposed to either air or oil[J]. Science, 2015, 347: 1132-1135.

[6] YARIN A L. Drop impact dynamics: Splashing, spreading, receding, bouncing[J]. Annual Review of Fluid Mechanics, 2006, 38: 159-192.

[7] LI Si, SHU Jun, ZHANG Zhiqiang, et al. Study on simulation for droplet mass distribution of supercooled large droplet cloud in icing wind tunnel[J]. Journal of Nanjing University of Aeronautics & Astronautics, 2023, 55(1): 146-153. (in Chinese)

[8] RICHARD D, CLANET C, QUÉRÉ D. Contact

time of a bouncing drop[J]. Nature, 2002, 417: 811.

[9] BIRD J C, DHIMAN R, KWON H M, et al. Reducing the contact time of a bouncing drop[J]. Nature, 2013, 503: 385-388.

[10] LIU Y, MOEVIUS L, XU X, et al. Pancake bouncing on superhydrophobic surfaces[J]. Nature Physics, 2014, 10: 515-519.

[11] SCHNEIDER J, EGATZ-GÓMEZ A, MELLE S, et al. Motion of viscous drops on superhydrophobic surfaces due to magnetic gradients[J]. Colloids and Surfaces A: Physicochemical and Engineering Aspects, 2008, 323: 19-27.

[12] TAKEDA K, NAKAJIMA A, HASHIMOTO K, et al. Jump of water droplet from a super-hydrophobic film by vertical electric field[J]. Surface Science, 2002, 519: L589-L592.

[13] QIN Y, LI X, JIAO K, et al. Effective removal and transport of water in a PEM fuel cell flow channel having a hydrophilic plate[J]. Applied Energy, 2014, 113: 116-126.

[14] JOSSERAND C, THORODDSEN S T. Drop impact on a solid surface[J]. Annual Review of Fluid Mechanics, 2016, 48: 365-391.

[15] MALOUIN B A, KORATKAR N A, HIRSA A H, et al. Directed rebounding of droplets by microscale surface roughness gradients[J]. Applied Physics Letters, 2010, 96: 234103.

[16] WANG L, LI J, ZHANG B, et al. Counterintuitive ballistic and directional liquid transport on a flexible droplet rectifier[J]. Research, 2021, 2020: 6472313.

[17] LIU C, LEGCHENKOVA I, HAN L, et al. Directional droplet transport mediated by circular groove arrays. Part I: Experimental findings[J]. Langmuir, 2020, 36(32): 9608-9615.

[18] LIU C, LEGCHENKOVA I, HAN L, et al. Directional droplet transport mediated by circular groove arrays. Part Ⅱ: Theory of effect[J]. Langmuir, 2021, 37(5): 1948-1953.

[19] FARSHCHIAN B, PIERCE J, BEHESHTI M S, et al. Droplet impinging behavior on surfaces with wettability contrasts[J]. Microelectronic Engineering, 2018, 195: 50-56.

[20] CHU F, LUO J, HAO C, et al. Directional transportation of impacting droplets on wettability-controlled surfaces[J]. Langmuir, 2020, 36: 5855-5862.

[21] SCHUTZIUS T M, GRAEBER G, ELSHARKAWY M, et al. Morphing and vectoring impacting droplets by means of wettability-engineered surfaces[J]. Scientific Reports, 2014, 4: 7029.

[22] ZHAO Z, LI H, HU X, et al. Steerable droplet bouncing for precise materials transportation[J]. Advanced Materials Interfaces, 2019, 6: 1901033.

[23] LI H, FANG W, LI Y, et al. Spontaneous droplets gyrating via asymmetric self-splitting on heterogeneous surfaces[J]. Nature Communication, 2019, 10: 950.

[24] RUSSO A, ICARDI M, ELSHARKAWY M, et al. Numerical simulation of droplet impact on wettability-patterned surfaces[J]. Physical Review Fluids, 2020, 5: 074002.

[25] ZHANG T, WU J, LIN X. Lateral motion of a droplet impacting on a wettability-patterned surface: Numerical and theoretical studies[J]. Soft Matter, 2021, 17: 724-737.

[26] ZHANG T, WU J, LIN X. Scaling laws for the droplet rebound with lateral motion after impacting on heterogeneous surfaces[J]. International Journal of Multiphase Flow, 2022, 148: 103960.

[27] ZHANG T, WU J, LIN X. An improved diffuse interface method for three-dimensional multiphase flows with complex interface deformation[J]. International Journal for Numerical Methods in Fluids, 2020, 92: 976-991.

[28] VAN DER WAALS J D. The thermodynamic theory of capillarity under the hypothesis of a continuous variation of density[J]. Journal of Statistical Physics, 1979, 20: 200-244.

[29] ZHOU L, HUANG P, ZHANG J. Phase field simulation of intragranular microvoids evolution due to surface diffusion in stress field[J]. Transactions of Nanjing University of Aeronautics and Astronautics, 2022, 39(3): 280-290.

[30] DING H, SPELT P D M, SHU C. Diffuse interface model for incompressible two-phase flows with large density ratios[J]. Journal of Computational Physics, 2007, 226: 2078-2095.

[31] KIM J. A continuous surface tension force formulation for diffuse-interface models[J]. Journal of Computational Physics, 2005, 204: 784-804.

[32] YUAN Z, MATSUMOTO M, KUROSE R. Directional migration of an impinging droplet on a surface with wettability difference[J]. Physical Review Fluids, 2020(5): 113605.

[33] KISTLER S F. Hydrodynamics of wetting[M]//Wettability. New York: Marcel Dekker, 1993: 311-430.

[34] YUAN Z, WEN J, MATSUMOTO M, et al. Anti-wetting ability of the hydrophobic surface decorated by submillimeter grooves[J]. International Journal of

Multiphase Flow, 2020, 131: 103404.
[35] LIU Y, TAN P, XU L. Kelvin-Helmholtz instability in an ultrathin air film causes drop splashing on smooth surfaces[J]. Proceedings of the National Academy of Sciences of the United States of America, 2015, 112: 3280-3284.
[36] MCGRAW J, LI J, TRAN D, et al. Plateau-Rayleigh instability in a torus: Formation and breakup of a polymer ring[J]. Soft Matter, 2010, 6: 1258-1262.

Acknowledgements This work was supported by the Foundation of National Key Laboratory of Science and Technology on Aerodynamic Design and Research (No. D5150230003), the Open Fund of Key Laboratory of Flight Techniques and Flight Safety, CAAC (No.FZ2021KF20), and the Priority Academic Program Development of Jiangsu Higher Education Institutions (PAPD).

Authors Dr. **ZHANG Tongwei** received the B.S. degree in mechanical engineering from Anhui University of Technology in 2015 and the Ph.D. degree in fluid mechanics from Nanjing University of Aeronautics and Astronautics in 2022, respectively. In June 2022, he joined the School of Automotive and Traffic Engineering, Jiangsu University, as a lecturer. His research is focused on multiphase flow, droplet manipulation, surface wettability and relevant fields.

Prof. **WU Jie** received the B. S. degree in aerodynamics from Nanjing University of Aeronautics and Astronautics in 2002 and the Ph.D. degree in fluid dynamics from National University of Singapore in 2010, respectively. He joined in Nanjing University of Aeronautics and Astronautics in February 2011, where he is currently a full professor and head of department of Aerodynamics. His research is focused on computational fluid dynamics and relevant fields.

Author contributions Dr. **ZHANG Tongwei** contributed to the conception of the study, performed the data analyses and wrote the manuscript. Dr. **KAKU Chuyo** interpreted the results and revised the manuscript. Ms. **LI Meixuan** contributed to the analyses and manuscript preparation. Prof. **WU Jie** helped perform the analyses with constructive discussion. All authors commented on the manuscript draft and approved the submission.

Competing interests The authors declare no competing interests.

(Production Editor: XU Chengting)

基于液滴定向反弹的混合润湿性表面设计准则

张童伟[1], KAKU Chuyo[2], 李美萱[3], 吴 杰[3,4]

(1.江苏大学汽车与交通工程学院,镇江 212013,中国; 2.江苏超力电器有限公司技术研究院,镇江 212321,中国; 3.南京航空航天大学航空学院,南京 210016,中国; 4.西北工业大学翼型、叶栅空气动力学国家级重点实验室,西安 710072,中国)

摘要:液滴撞击固体表面的定向反弹在防结冰/起雾、自清洁等工程应用中具有重要意义。混合润湿性表面已被证明是一种有效的液滴操纵方法。本文对液滴撞击构筑有亲水条纹的疏水基底进行数值模拟研究,采用已验证的扩散界面法来捕获界面演化。首先,研究卫星液滴在撞击过程中的形成过程,通过分析液滴的垂直速度和横向速度,明确混合润湿性表面在液滴扩散、收缩和反弹阶段中的作用。然后,系统探究条纹宽度对液滴反弹形式和接触时间的影响,重点关注液膜演化和液滴弹跳过程中的动力学和能量传递机制。所得结果可以指导混合润湿性表面的优化设计和液滴定向回弹的控制。

关键词:液滴撞击;混合润湿性表面;定向反弹;设计准则